Area of overlap and interference in phase space versus Wigner pseudoprobabilities

W. Schleich
Max-Planck-Institut für Quantenoptik, D-8046 Garching bei München, Federal Republic of Germany and Department of Physics, University of Texas–Austin, Austin, Texas 78712

D. F. Walls
Department of Physics, University of Auckland, Auckland, New Zealand

J. A. Wheeler
Department of Physics, University of Texas–Austin, Austin, Texas 78712

(Received 26 January 1988)

In the semiclassical approximation, the quantum-mechanical scalar product between two quantum states is governed by (1) the areas of overlap in phase space of these states and (2) *interference* between the probability amplitudes contributed by these areas. We compare and contrast this principle with Wigner's concept of pseudoprobabilities in phase space and illustrate the essential points of both treatments by the oscillations in the photon distribution of a highly squeezed state.

I. INTRODUCTION AND OVERVIEW

The double-slit experiment[1] summarizes most clearly the central lesson of quantum mechanics: Probabilities at the microscopic level are governed by interfering probability amplitudes[2] rather than by additive probabilities. In the semiclassical limit[3] (Bohr's correspondence principle[4]) these interfering probability amplitudes are interfering areas in phase space.[5] We ask here how this very concept of *interference in phase space*[5] compares and contrasts to Wigner's celebrated approach[6] of performing quantum-mechanical calculations in phase space using distribution functions.[7]

The area-of-overlap plus interference concept[5] identifies two (or more) well-defined zones of crossover in phase space as contributors of probability amplitude, and further identifies an entire domain in phase space as the determiner of the phase difference between these amplitudes. In contrast, the Wigner approach[6,7] deals with the probabilities themselves, and these probabilities—some positive, some negative ("pseudoprobabilities")—contribute to every domain in phase space. We shall see how these apparently totally different algorithms for calculating transition probability give insight into each other.

For this purpose we have chosen the example of the photon distribution W_m of a highly squeezed state of the electromagnetic field.[8] In such a nonclassical state[9] the uncertainty in one of the two dynamically conjugate field variables x and p is less than the corresponding one in a coherent state.[10] As a consequence of interference in phase space, the photon-count probability W_m of such a state exhibits—for an appropriate choice of parameters—the oscillations[11] depicted in Fig. 1.

These two concepts do not exhaust the possibilities to interpret the oscillations in W_m as a consequence of interference in phase space. A different approach[12] uses a phase-integral representation of a number state in terms of coherent states. In this theory the interference appears to originate from the fact that the phase-space integral runs over an oscillatory amplitude function closely related to the Q function,[6] a phase-space distribution function different from Wigner's.

The article is organized as follows. In Sec. II we obtain the oscillations in the photon distribution W_m of a highly

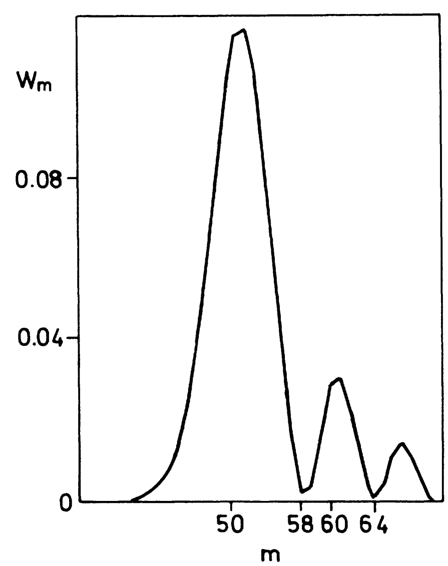

FIG. 1. Probability W_m of finding m photons in a highly squeezed state, Eq. (2.1), is an oscillatory function for quantum numbers m appropriately larger than the displacement α^2. (Squeezing parameter $\epsilon=0.1$ and $\alpha^2=49$. Curves, it should be recognized, are not really continuous curves, because m is never other than an integer.)

squeezed state from a semiclassical analysis of the quantum-mechanical scalar product. The amplitude $\mathcal{A}_m$ and the phase ϕ_m of these oscillations are related in Sec. III to the area of overlap A_m in phase space between the mth number state and the squeezed state and to the area caught between the center lines of the two states, respectively. In Sec. IV we evaluate W_m within the formalism of the Wigner function. We show that the outermost and highest-amplitude wave crest of the Wigner function[13] $P_m^{(w)}$, of the mth number state cuts out of the Gaussian cigar of the squeezed state an area equal to that of the area-of-overlap algorithm. The inner wave crests and troughs of $P_m^{(w)}$ have lower amplitude. The troughs create "ditches" in phase space—the origin of the oscillatory behavior of W_m. Section V provides a summary and conclusion. In order to focus on the central points we have banished all lengthy calculations to appendixes.

II. OSCILLATIONS IN THE PHOTON-COUNT PROBABILITY W_m OF A HIGHLY SQUEEZED STATE VIA THE QUANTUM-MECHANICAL SCALAR PRODUCT

The most striking feature of a highly squeezed state—the oscillatory[11] photon distribution W_m shown in Fig. 1—will serve in the following sections an an example in the comparison between the concept of interference in phase space[5] and the corresponding Wigner-function treatment. We therefore present in this section a simple semiclassical derivation of this rapid variation of W_m.

According to the standard rules of quantum mechan-

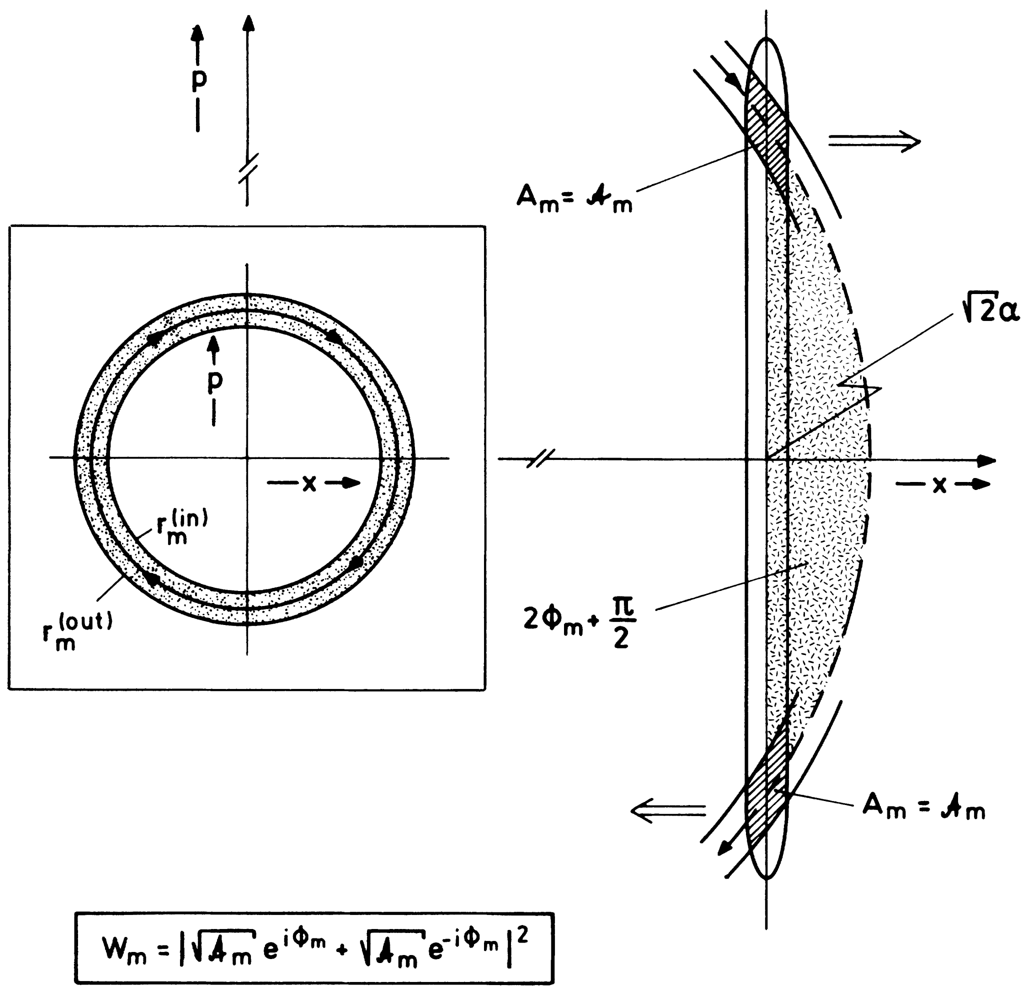

FIG. 2. Oscillations in photon distribution of a highly squeezed state as a consequence of *interference in phase space.* For excitations m appropriately larger than α^2 the bands of inner radius $r_m^{(\mathrm{in})}=(2m)^{1/2}$ and outer radius $r_m^{(\mathrm{out})}=[2(m+1)]^{1/2}$ shown in the inset and representing the mth number state intersect the elliptical contour line of a highly squeezed state in two symmetrically located diamond-shaped zones of weighted area $A_m=\mathcal{A}_m$. The field oscillator traverses the band in the clockwise direction, as indicated in the inset. Therefore in one zone the oscillator is moving to the "right;" in the other, to the "left." The total probability amplitude $\sqrt{W_m}$ is thus the sum of contributions $\sqrt{\mathcal{A}_m}\exp(\pm i\phi_m)$ from the shaded areas. The phase ϕ_m is fixed by the dotted area caught between the center lines of the two states. As a result of this *interference in phase space* the photon distribution W_m is oscillatory for m values appropriately larger than α^2.

ics[14] the probability W_m of finding m photons in a highly squeezed state[15]

$$\psi_{sq}(x)=(2/\pi\epsilon)^{1/4}\exp[-(1/\epsilon)(x-\sqrt{2}\alpha)^2] , \quad (2.1)$$

with squeeze parameter ϵ (where $0<\epsilon\ll 1$) and shift parameter α, is given by

$$W_m = w_m^2 , \quad (2.2a)$$

where

$$w_m=(2/\pi\epsilon)^{1/4}\int_{-\infty}^{\infty} dx\, u_m(x) e^{-(1/\epsilon)(x-\sqrt{2}\alpha)^2} . \quad (2.2b)$$

Here

$$u_m(x)=\pi^{-1/4}(2^m m!)^{-1/2}H_m(x)e^{-x^2/2} \quad (2.3)$$

denotes the wave function of the mth number state.[14]

With the help of Eq. (A3) of Appendix A, Eq. (2.2b) reads

$$w_m=(2\pi\epsilon)^{1/4}\sum_{k=0}^{\infty}\frac{(\epsilon/4)^k}{k!}\frac{d^{2k}u_m(x)}{dx^{2k}}\bigg|_{x=\sqrt{2}\alpha} . \quad (2.4)$$

For $|x|$ appropriately smaller than $\xi_m \equiv [2(m+\frac{1}{2})]^{1/2}$ we approximate $u_m = u_m(x)$ of Eq. (2.3) by the familiar Wentzel-Kramers-Brillouin (WKB) wave functions[3]

$$u_m(x) \cong (2/\pi)^{1/2}[p_m(x)]^{-1/2}\cos[S_m(x)-\pi/4] , \quad (2.5)$$

where

$$p_m(x)=[2(m+\tfrac{1}{2})-x^2]^{1/2} \quad (2.6)$$

and

$$S_m(x)=\int_x^{\xi_m} dx'\, p_m(x') . \quad (2.7)$$

When we differentiate u_m we neglect the slow variation of $[p_m(x)]^{-1/2}$ compared to $\cos(S_m-\pi/4)$ and find

$$\frac{d^{2k}u_m(x)}{dx^{2k}} \cong (-1)^k [p_m(x)]^{2k} u_m(x) .$$

We substitute this result back into Eq. (2.4) and perform the summation, which together with Eqs. (2.2a), (2.5), (2.6) and (2.7) yields

$$W_m \cong 4\mathcal{A}_m \cos^2\phi_m , \quad (2.8a)$$

where

$$\mathcal{A}_m = \left[\frac{\epsilon}{4\pi}\right]^{1/2} \frac{e^{-\epsilon(m+1/2-\alpha^2)}}{(m+\frac{1}{2}-\alpha^2)^{1/2}} \quad (2.8b)$$

and

$$\phi_m = S_m(x=\sqrt{2}\alpha)-\frac{\pi}{4} = \int_{\sqrt{2}\alpha}^{\xi_m} dx\, p_m(x) - \frac{\pi}{4} . \quad (2.8c)$$

As a consequence of the previously mentioned validity condition for the WKB wave function, Eq. (2.5), Eq. (2.8) describes the photon statistics of W_m only in the limit of quantum numbers m appropriately larger than $\alpha^2 \gg 1$, that is, in the oscillatory region—the center of interest of this paper. For a detailed discussion of the behavior of W_m in other regimes of m we refer to Ref. 11.

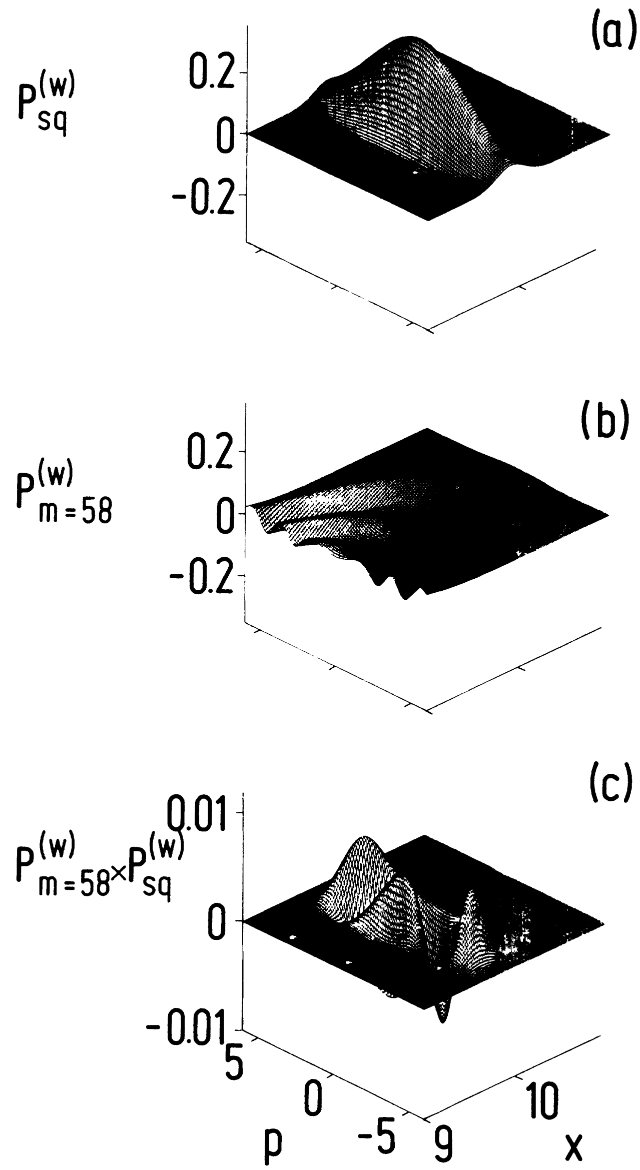

FIG. 3. In the framework of the Wigner function formalism the probability $W_{m=58}$ of finding $m=58$ photons in a highly squeezed state [Gaussian cigar of (a)] is obtained by integrating the product $P_{m=58}^{(w)}P_{sq}^{(w)}$ of the corresponding Wigner functions (c) over phase space. In complete correspondence to the $m=58$th Bohr-Sommerfeld band of Fig. 2 the outermost wave front of the oscillator Wigner function $P_{m=58}^{(w)}$, (b), cuts out of the Gaussian cigar two symmetrically located peaks similar to the two diamond-shaped zones of Fig. 2. Moreover, the area W_m^{diam}, underneath each of these peaks is equal to the area $A_m = \mathcal{A}_m$ of one of the weighted diamonds. The next inner wave front of $P_{m=58}^{(w)}$ exhibits negative values and creates a "ditch" in phase space and in the product $P_{m=58}^{(w)}P_{sq}^{(w)}$. The following wave front with positive values gives rise to the "tongue," of (c). The weighted area of the "ditch" and the "tongue," W_m^{ditch}, is given by Eq. (4.6′), $W_m^{\text{ditch}} \cong 2\mathcal{A}_m\cos(2\phi_m)$, which results in the photon count probability $W_m = 2W_m^{\text{diam}} + W_m^{\text{ditch}} \cong 2\mathcal{A}_m + 2\mathcal{A}_m\cos(2\phi_m)$. For $m=58$ we find roughly as many positively as negatively weighted areas and thus $W_{m=58}\cong 0$, in agreement with Fig. 1 (here we have chosen $\alpha^2=49$ and $\epsilon=0.1$).

III. OSCILLATIONS IN W_m AS A RESULT OF INTERFERENCE IN PHASE SPACE

In this section we show that Eq. (2.8) allows a simple geometrical interpretation in phase space and, in particular, that the oscillations in W_m are a consequence of interference in phase space. In the semiclassical limit[3] the mth number state, described by the WKB wave function u_m of Eq. (2.5), can be represented in phase space as a circular Bohr-Sommerfeld band[16] of area 2π (in units $\hbar$) with inner radius[5] $r_m^{(\text{in})}=(2m)^{1/2}$ and outer radius $r_m^{(\text{out})}=[2(m+1)]^{1/2}$, as shown in the inset of Fig. 2. The Bohr-Sommerfeld trajectory, Eq. (2.6)

$$m+\tfrac{1}{2}=(1/2)p_m^2+(1/2)x^2 , \tag{3.1}$$

runs in the middle of the band.

For excitations m appropriately larger than α^2 each band intersects the elliptical contour line of the Gaussian cigar

$$P_{\text{sq}}^{(w)}(x,p)=\pi^{-1}e^{-(2/\epsilon)(x-\sqrt{2}\alpha)^2}e^{-(\epsilon/2)p^2} \tag{3.2}$$

representing the Wigner-Cohen function[6,7] of a highly squeezed state [shown in Fig. 3(a)] in two symmetrically located diamond-shaped zones. Each zone has the weighted area

$$A_m=\tfrac{1}{2}\int dx \int_{m\text{th band}} dp P_{\text{sq}}^{(w)}(x,p)\cong\mathcal{A}_m . \tag{3.3}$$

In the last step we have performed the integration shown in detail in Appendix B. Hence the area A_m of one of the diamonds is identical to the amplitude $\mathcal{A}_m$, Eq. (2.8b), of the oscillations.

The probability W_m to find m photons in a highly squeezed state is not, however, the sum $2A_m$ of the areas of the two diamonds. Neither is the intensity on the photographic plate in the familiar double-split experiment[1] equal to the sum of intensities that would arrive through the two slits separately.

Quantum mechanics instructs us to add not probabilities but probability amplitudes.[2] The absolute value of the probability amplitude corresponding to one diamond is obviously $(A_m)^{1/2}=(\mathcal{A}_m)^{1/2}$. The Bohr-Sommerfeld band is traversed in the clockwise direction as indicated in Fig. 2. In one diamond the field oscillator is thus moving to the "right," whereas in the other it is moving to the "left," which yields

$$W_m=|\sqrt{\mathcal{A}_m}e^{i\phi_m}+\sqrt{\mathcal{A}_m}e^{-i\phi_m}|^2 , \tag{3.4}$$

a result identical to Eq. (2.8). According to Eq. (2.8c) the interference-fixing phase

$$\phi_m=(1/2)\int_{\sqrt{2}\alpha}^{\xi_m}dx\int_{-p_m}^{p_m}dp-\pi/4 \tag{3.5}$$

is (aside from the constant phase shift $\pi/4$) given by half the area caught between the center lines [Eq. (3.1) and $x=\sqrt{2}\alpha$] of the two states, as indicated in Fig. 2.

IV. OSCILLATIONS IN W_m AS A RESULT OF NEGATIVE WIGNER PSEUDOPROBABILITIES

We now compare and contrast the concept of interference in phase space[5] to the corresponding Wigner-function treatment. In this formalism the probability W_m of Eq. (2.2) is given[17] by

$$W_m=2\pi\int_{-\infty}^{\infty}dx\int_{-\infty}^{\infty}dp\, P_m^{(w)}(x,p)P_{\text{sq}}^{(w)}(x,p) , \tag{4.1}$$

where $P_{\text{sq}}^{(w)}$ denotes the Wigner function of the squeezed state [Eq. (3.2)] and $P_m^{(w)}$ is the Wigner function of the harmonic oscillator[6,13] in its mth state of excitation,

$$P_m^{(w)}(x,p)=(-1)^m\pi^{-1}\exp[-(x^2+p^2)]L_m[2(x^2+p^2)] . \tag{4.2}$$

Here L_m is the mth Laguerre polynomial.[18,19] The probability W_m is thus given by the overlap in phase space [Fig. 3(c)] between the distributions $P_{\text{sq}}^{(w)}$, Eq. (3.2), shown in Fig. 3(a) and $P_m^{(w)}$, Eq. (4.2), shown in Fig. 3(b) in the neighborhood of the Gaussian cigar of the squeezed state. In order to make contact with and stress the relation to the area-of-overlap approach we again perform the phase-space integration of Eq. (4.1) in the semiclassical limit,[20] that is, for large displacements $\alpha^2\gg 1$. Moreover, we consider strong squeezing, that is, $0<\epsilon\ll 1$. We treat the general case in Appendix C.

The exponential falloff of the Gaussian cigar of the squeezed state confines the phase-space integration to an ellipse of height $(2/\epsilon)^{1/2}$ and width $(\epsilon/2)^{1/2}$ centered on the positive x axis at $x=\sqrt{2}\alpha$, as shown in Fig. 3(c). The Wigner function $P_m^{(w)}$, Eq. (4.2), consists[13,21] of spherical waves emerging from the origin of phase space with the outermost feature always being a crest[20,21] located in the neighborhood of the Bohr-Sommerfeld trajectory, Eq. (3.1), as shown in Fig. 3(b). This outermost wave crest cuts out of the cigar $P_{\text{sq}}^{(w)}$ two symmetrically located peaks, whereas the inner wave troughs and crests create the "ditches" and "tongues" in phase space, shown in Fig. 3(c). We therefore decompose the phase-space integration, Eq. (4.1), into

$$W_m=2W_m^{\text{diam}}+W_m^{\text{ditch}} \tag{4.3}$$

("diamonds" plus "ditches"), where

$$W_m^{\text{diam}}=(2/\pi)\int_{-\infty}^{\infty}dx\int_{\bar{p}_m(x)}^{\infty}dp(-1)^m e^{-(x^2+p^2)}L_m[2(x^2+p^2)]e^{-(\epsilon/2)p^2}e^{-(2/\epsilon)(x-\sqrt{2}\alpha)^2} \tag{4.4a}$$

is the weighted value of the diamondlike area underneath *one* of the symmetrical peaks and

$$W_m^{\text{ditch}}=(2/\pi)\int_{-\infty}^{\infty}dx\int_{-\bar{p}_m(x)}^{\bar{p}_m(x)}dp(-1)^m e^{-(x^2+p^2)}L_m[2(x^2+p^2)]e^{-(\epsilon/2)p^2}e^{-(2/\epsilon)(x-\sqrt{2}\alpha)^2} \tag{4.4b}$$

is the weighted value of the area underneath the "ditch" and "tongue." Here $\tilde{p}_m=(\rho_m/2-x^2)^{1/2}$ and ρ_m denotes the largest zero[18] of the mth Laguerre polynomial.

In the two symmetrically located peaks of Fig. 3(c) the Gaussian cigar acts like a δ function

$$e^{-(2/\epsilon)(x-\sqrt{2}\alpha)^2}\cong(\epsilon\pi/2)^{1/2}\delta(x-\sqrt{2}\alpha) \tag{4.5}$$

in x space, and thus

$$W_m^{\text{diam}}\cong(2\epsilon/\pi)^{1/2}\int_{\tilde{p}_m(x=\sqrt{2}\alpha)}^{\infty}dp(-1)^m e^{-[(\sqrt{2}\alpha)^2+p^2]}L_m\{2[(\sqrt{2}\alpha)^2+p^2]\}e^{-(\epsilon/2)p^2}\ .$$

When we evaluate the slowly varying exponential function $e^{-\epsilon p^2/2}$ at the Bohr-Sommerfeld trajectory $p_m^2=2(m+\frac{1}{2})-2\alpha^2\cong\tilde{p}_m^{\,2}(x=\sqrt{2}\alpha)$, we find

$$W_m^{\text{diam}}\cong(2\epsilon/\pi)^{1/2}e^{-\epsilon(m+1/2-\alpha^2)}\times\int_{\tilde{p}_m(x=\sqrt{2}\alpha)}^{\infty}dp(-1)^m e^{-[(\sqrt{2}\alpha)^2+p^2]}\times L_m\{2[(\sqrt{2}\alpha)^2+p^2]\}\ .$$

The remaining integration has been performed in Appendix D. With the help of Eq. (D3) we arrive at

$$W_m^{\text{diam}}\simeq\left[\frac{\epsilon}{4\pi}\right]^{1/2}\frac{e^{-\epsilon(m+1/2-\alpha^2)}}{(m+\frac{1}{2}-\alpha^2)^{1/2}}=A_m\simeq\mathcal{A}_m\ . \tag{4.6}$$

Thus the weighted value of the area underneath one of the two symmetrically located peaks of Fig. 3(c) is equal in the appropriate limit to the weighted area A_m of one of the diamond-shaped zones of the Bohr-Sommerfeld area-of-overlap formalism. This equivalence is analogous to the corresponding equivalence[21] of the photon-count probability of a coherent state.[10] There the contribution from the outermost crest of the Wigner function is equivalent[21] to the contribution from the mth Bohr-Sommerfeld band. For such a coherent state, moreover, the inner crests and troughs of $P_m^{(w)}$ do not contribute significantly[21] to the photon statistics. However, in the present case of a squeezed state they give rise to the oscillatory behavior of W_m. This we shall now demonstrate. We therefore turn to the calculation of the weighted value of the area covered by the "tongue" and the "ditch;" that is, of the W_m^{ditch} of Eq. (4.4b).

We first perform the integration over p and neglect the slight falloff of the cigar with increasing p along $x=$const, that is, we set $\exp[-(\epsilon/2)p^2]\cong 1$,

$$W_m^{\text{ditch}}\cong(2/\pi)\int_{-\infty}^{\infty}dx\left[\int_{-\tilde{p}_m}^{\tilde{p}_m}dp(-1)^m e^{-(x^2+p^2)}\times L_m[2(x^2+p^2)]\right]\times e^{-(2/\epsilon)(x-\sqrt{2}\alpha)^2}\ .$$

The integration over p can then be performed with the help of Eq. (D6), that is,

$$W_m^{\text{ditch}}\cong(2/\pi)[2(m+\tfrac{1}{2})-2\alpha^2]^{-1/2}\times\int_{-\infty}^{\infty}dx\cos[2S_m(x)-\pi/2]\times\exp[-(2/\epsilon)(x-\sqrt{2}\alpha)^2]\ ,$$

where we have evaluated the slowly varying function $[p_m(x)]^{-1}$ arising from Eq. (D6) at $x=\sqrt{2}\alpha$ and factored it out of the integral. With the help of Appendix A, Eq. (A3), the preceding integral can be expressed as a power series in ϵ

$$W_m^{\text{ditch}}\cong(\epsilon/\pi)^{1/2}\frac{1}{(m+\frac{1}{2}-\alpha^2)^{1/2}}\times\sum_{k=0}^{\infty}\frac{(\epsilon/8)^k}{k!}\times\frac{d^{2k}}{dx^{2k}}\{\cos[2S_m(x)-\pi/2]\}\,|_{x=\sqrt{2}\alpha}\ . \tag{4.7}$$

When we neglect the slow variation of $p_m(x)$ compared to $\cos(2S_m-\pi/2)$, we can evaluate the derivative

$$\frac{d^{2k}}{dx^{2k}}\{\cos[2S_m(x)-\pi/2]\}\cong(-4)^k[p_m(x)]^{2k}\cos[2S_m(x)-\pi/2]\ ,$$

and thus reduce Eq. (4.7) to

$$W_m^{\text{ditch}}\cong 2\left[\frac{\epsilon}{4\pi}\right]^{1/2}\frac{1}{(m+\frac{1}{2}-\alpha^2)^{1/2}}\times\sum_{k=0}^{\infty}\frac{[(-\epsilon)(m+\frac{1}{2}-\alpha^2)]^k}{k!}\cos(2\phi_m)=2\mathcal{A}_m\cos(2\phi_m)\ . \tag{4.6$'$}$$

Therefore the oscillatory behavior of W_m is contained in the "ditches" of the product $P_m^{(w)}P_{\text{sq}}^{(w)}$ of Fig. 3(c) caused by the inner wave troughs of $P_m^{(w)}$ with their negative values. This is confirmed by Fig. 4, where we show this product for $m=60$ and 64. Here the inner wave troughs reach deeper into the cigar, forming ditches with a depth different from the $m=58$ case and therefore giving rise to the oscillations in W_m. We conclude this section by substituting Eqs. (4.6) and (4.6′) back into Eq. (4.3) to find

$$W_m = 2\mathcal{A}_m + 2\mathcal{A}_m \cos(2\phi_m) , \tag{4.8}$$

a result identical to Eq. (2.8).

V. SUMMARY AND CONCLUSIONS

In summary, we emphasize the similarities and differences between the concept of interference in phase space and the Wigner-function formalism when applied to the example of the photon-count probability W_m of a highly squeezed state. In complete correspondence to the mth Bohr-Sommerfeld band the outermost wave crest of the Wigner function of the mth number state cuts out of the long, thin, Gaussian cigar of the squeezed state two symmetrically located peaks with diamond-shaped contour lines and weighted area W_m^{diam} Eq. (4.6), equal to the corresponding area A_m, Eq. (3.3), of the area-of-overlap algorithm. The rapid variation in W_m appears as a consequence of *interference* between the two peaks, Eq. (3.4). In the framework of the Wigner function, however, these beats arise from areas in phase space in which the Wigner function of the mth number state attains negative values, that is, from the inner wave troughs. Moreover, in the area-of-overlap approach the interference-fixing phase ϕ_m is governed by the area caught between the center lines of the mth Bohr-Sommerfeld band and the squeezed state cigar and thus by an area in phase space *outside* of the cigar. This is in contrast to the Wigner equivalent where the *total* expression $2\mathcal{A}_m \cos(2\phi_m)$ is determined, Eq. (4.6′), by the "ditches" and "tongues" created by the inner wave troughs and crests *within* the cigar. The main difference between the two concepts, however, stands out most clearly in a direct comparison between Eqs. (3.4) and (4.8): The area-of-overlap plus interference concept identifies two (or more) well-defined zones of crossover in phase space as contributors of probability *amplitude*. In contrast, the Wigner approach deals with *probabilities* themselves—some positive and some negative ("pseudoprobabilities")—to account for interference phenomena.

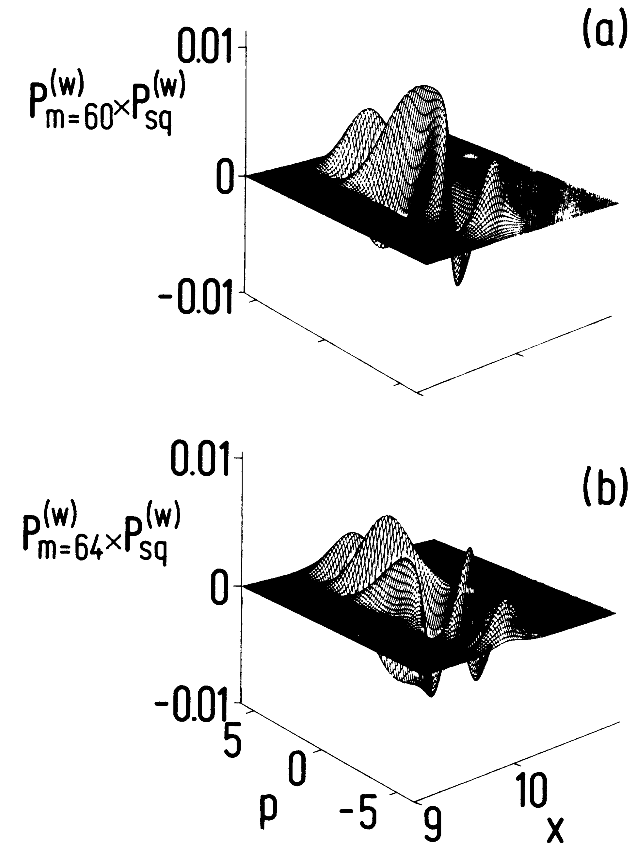

FIG. 4. When the field oscillator is in its $m = 60$th state of excitation, the wave fronts have progressed further outwards compared to the $m = 58$th state. Again the outermost band cuts out two symmetrically located peaks, each of weighted area $A_m = \mathcal{A}_m$. However, the following wave front with positive value now reaches deeper into the Gaussian cigar thus amplifying the "tongue" and reducing the depth of the "ditch," as shown in (a). Consequently, integration over phase space yields an unusually large value for $W_{m=60}$, in agreement with Fig. 1. This inner wave front has marched even further outwards for the $m = 64$th state as to cut the Gaussian cigar twice. Only a small "tongue" survives from the next wave front with positive values. Therefore integration over phase space results in an almost vanishing probability $W_{m=64}$ as shown in Fig. 1. This clearly demonstrates that the oscillations in the photon distribution of a highly squeezed state result from the inner negative-valued wave fronts of the Wigner function for the oscillator. (Here, as in the other figures, we have chosen $\alpha^2 = 49$ and $\epsilon = 0.1$.)

In conclusion, we note that standard quantum mechanics provides the probability to find m photons in a squeezed state in the shape of Eq. (2.2),

$$W_m = w_m^2 = \int_{-\infty}^{\infty} dx \int_{-\infty}^{\infty} d\mathcal{X}\, \psi_{\text{sq}}(x)\psi_{\text{sq}}(\mathcal{X}) u_m(x) u_m(\mathcal{X}) . \tag{5.1}$$

Yet hardly from this formula by mere unmotivated calculation would the discovery have been made that the photon distribution of a highly squeezed state undergoes oscillations. That insight came out of the semiclassical analysis[11] of Sec. III, not out of Eq. (5.1). Moreover, the semiclassical analysis provides a quick and simple way to get results that are approximate but often quite good approximations. Therefore the motive is strong to provide a link between Eq. (5.1)—expressed here as a double integral—and the semiclassical analysis. That link we now have in the results of this paper. The reasoning leads from the integrals, Eq. (5.1), in x and $\mathcal{X}$ space to a Fourier transform in x,p space—the Wigner function. This correspondence is here and now spelled out with the area of overlap in phase space.

ACKNOWLEDGMENTS

The authors thank L. Cohen, J. P. Dahl, K. Dodson, P. Drummond, R. Glauber, M. Hillery, J. Kimble, K. Kraus, R. F. O'Connell, and M. O. Scully for useful and stimulating discussions. In particular, we thank M. Brown and C.-S. Cha for the computer evaluation of the curves shown here. Preparation of this article was assisted by the University of Texas at Austin and by the National Science Foundation Grant No. PHY 850 3890.

APPENDIX A: EXPRESSION FOR INTEGRAL EQ. (2.2b) IN TERMS OF A POWER SERIES

In this appendix we express the integral

$$\omega=\int_{-\infty}^{\infty} dx\, f(x)e^{-(1/\lambda)(x-\sqrt{2}\alpha)^2} \tag{A1}$$

for functions f which allow the Taylor expansion

$$f(x)=\sum_{k=0}^{\infty}\frac{1}{k!}\frac{d^kf}{dx^k}\bigg|_{x=\sqrt{2}\alpha}(x-\sqrt{2}\alpha)^k \tag{A2}$$

in a power series of λ. When we substitute Eq. (A2) into Eq. (A1),

$$w=\sum_{k=0}^{\infty}\frac{1}{k!}\frac{d^kf}{dx^k}\bigg|_{x=\sqrt{2}\alpha}\times\int_{-\infty}^{\infty}dx(x-\sqrt{2}\alpha)^k e^{-(1/\lambda)(x-\sqrt{2}\alpha)^2},$$

we can perform the resulting integrations with the help[22] of

$$\int_{-\infty}^{\infty}dy\, e^{-y^2/\lambda}y^{2k+1}=0$$

and

$$\int_{-\infty}^{\infty}dy\, e^{-y^2/\lambda}y^{2k}=\pi^{1/2}\lambda^{k+1/2}2^{-2k}(2k)!/k!$$

to yield

$$\omega=(\pi\lambda)^{1/2}\sum_{k=0}^{\infty}\frac{(\lambda/4)^k}{k!}\frac{d^{2k}f}{dx^{2k}}\bigg|_{x=\sqrt{2}\alpha}. \tag{A3}$$

APPENDIX B: AREA OF OVERLAP BETWEEN GAUSSIAN CIGAR AND MTH BOHR-SOMMERFELD BAND

In this appendix we calculate the area of overlap

$$2A_m=\int_{m\text{th band}} dx\int dp\, P_{\rm sq}^{(w)}(x,p) \tag{B1}$$

between the mth band defined by the edges $r_m^{(\rm in)}=(2m)^{1/2}$ and $r_m^{(\rm out)}=[2(m+1)]^{1/2}$ and the long, thin Gaussian cigar

$$P_{\rm sq}^{(w)}(x,p)=(1/\pi)e^{-(2/\epsilon)(x-\sqrt{2}\alpha)^2-(\epsilon/2)p^2}, \tag{B2}$$

representing a highly squeezed state ($0<\epsilon\ll 1$). When we substitute Eq. (B2) into Eq. (B1) and note that for $0<\epsilon\ll 1$

$$(2/\pi\epsilon)^{1/2}e^{-(2/\epsilon)(x-\sqrt{2}\alpha)^2}\cong\delta(x-\sqrt{2}\alpha),$$

we can perform the integration with respect to x and arrive at

$$\begin{aligned}2A_m&\cong 2(\epsilon/2\pi)^{1/2}\int_{(2m-2\alpha^2)^{1/2}}^{[2(m+1)-2\alpha^2]^{1/2}}dp\,\exp(-\epsilon p^2/2)\\&\cong 2(\epsilon/2\pi)^{1/2}\{[2(m+1)-2\alpha^2]^{1/2}-[2m-2\alpha^2]^{1/2}\}\exp[-(\epsilon/2)((1/2)\{[2(m+1)-2\alpha^2]^{1/2}+(2m-2\alpha^2)^{1/2}\})^2]\,.\end{aligned} \tag{B3}$$

Here we have confined the integration to one of the two symmetrically located diamond-shaped zones of Fig. 2. Moreover, in the last step we have approximated the integral by its width times the value of the integrand at the center of the interval.

With the help of[21]

$$\begin{aligned}(m+1-\alpha^2)^{1/2}-(m-\alpha^2)^{1/2}&=\frac{(m+1-\alpha^2)-(m-\alpha^2)}{(m+1-\alpha^2)^{1/2}+(m-\alpha^2)^{1/2}}\\&\cong\frac{1}{2(m+\frac{1}{2}-\alpha^2)^{1/2}},\end{aligned}$$

Eq. (B3) reduces to

$$A_m\cong\left[\frac{\epsilon}{4\pi}\right]^{1/2}\frac{e^{-\epsilon(m+\frac{1}{2}-\alpha^2)}}{(m+\frac{1}{2}-\alpha^2)^{1/2}}=\mathcal{A}_m\,.$$

We get an approximate but simple check of the reasonableness of this result by testing whether the probabilities W_m of Eq. (2.8a) add to unity,

$$\begin{aligned}\sum_m W_m&\cong\int dm\, 4\mathcal{A}_m\cos^2\phi_m\\&\cong 2\int dm\,\mathcal{A}_m\\&=\int_0^{\infty}dm'(\epsilon/\pi)^{1/2}\frac{e^{-\epsilon m'}}{(m')^{1/2}}=1\quad(m'\equiv m+\tfrac{1}{2}-\alpha^2)\,.\end{aligned}$$

APPENDIX C: PHOTON DISTRIBUTION OF SQUEEZED STATES VIA WIGNER FUNCTION

In this appendix we perform the phase-space integration

$$W_m=2\pi\int_{-\infty}^{\infty}dx\int_{-\infty}^{\infty}dp\, P_m^{(w)}(x,p)P_{\rm sq}^{(w)}(x,p) \tag{C1}$$

to obtain the photon distribution of a squeezed state located at the positive x axis at $x_0=\sqrt{2}\alpha$ and represented by its Wigner function

$$P_{\rm sq}^{(w)}(x,p)=\pi^{-1}\exp[-s(x-\sqrt{2}\alpha)^2-p^2/s]\,. \tag{C2}$$

When we substitute the Wigner function of a harmonic oscillator in its mth state,[6,13]

$$P_m^{(w)}(x,p)=(-1)^m\pi^{-1}\exp(-x^2-p^2)L_m[2(x^2+p^2)]\,,$$

together with Eq. (C2) into Eq. (C1), we find after minor algebra

$$W_m=(2/\pi)(-1)^m\exp\left[-\frac{2s}{s+1}\alpha^2\right]\int_{-\infty}^{\infty}dx\int_{-\infty}^{\infty}dp\,\exp\left[-\left[(s+1)^{1/2}x-\frac{s\sqrt{2}\alpha}{(s+1)^{1/2}}\right]^2\right]\times\exp\left[-\left[\frac{s+1}{s}\right]p^2\right]L_m[2(x^2+p^2)] \tag{C3}$$

The relation[23]

$$L_m[2(x^2+p^2)]=(-1)^m2^{-2m}\sum_{k=0}^{m}\frac{1}{k!(m-k)!}H_{2(m-k)}(2^{1/2}x)H_{2k}(2^{1/2}p)$$

allows us to decouple the x and p integration in Eq. (C3), which then reads

$$W_m=\pi^{-1}2^{-(2m-1)}\exp\left[-\frac{2s}{s+1}\alpha^2\right]\frac{s^{1/2}}{s+1}\sum_{k=0}^{m}\frac{1}{k!(m-k)!}\int_{-\infty}^{\infty}d\kappa\exp\left[-\left[\kappa-\frac{s\sqrt{2}\alpha}{(s+1)^{1/2}}\right]^2\right]H_{2(m-k)}\left[\left[\frac{2}{s+1}\right]^{1/2}\kappa\right]\times\int_{-\infty}^{\infty}d\zeta\,e^{-\zeta^2}H_{2k}\left[\left[\frac{2s}{s+1}\right]^{1/2}\zeta\right]. \tag{C4}$$

Here we have introduced the new integration variables

$$\kappa\equiv(s+1)^{1/2}x \text{ and } \zeta\equiv[(s+1)/s]^{1/2}p .$$

The remaining two integrals can be found in Ref. 22 as

$$\int_{-\infty}^{\infty}dy\,e^{-(y-z)^2}H_k(\lambda y)=\pi^{1/2}(1-\lambda^2)^{k/2}H_k\left[\frac{\lambda}{(1-\lambda^2)^{1/2}}z\right]$$

and

$$\int_{-\infty}^{\infty}dy\,e^{-y^2}H_{2k}(\lambda y)=\pi^{1/2}\frac{(2k)!}{k!}(\lambda^2-1)^k .$$

They simplify Eq. (C4) to

$$W_m=\frac{2\sqrt{s}}{s+1}\left[\frac{s-1}{s+1}\right]^m2^{-2m}\times\sum_{k=0}^{m}\frac{(2k)!}{(k!)^2(m-k)!}H_{2(m-k)}\left[\frac{s}{(s^2-1)^{1/2}}2\alpha\right]\times\exp\left[-\frac{2s}{s+1}\alpha^2\right].$$

With the help of[24]

$$\frac{m!}{2^m}\sum_{j=0}^{m}\frac{[2(m-j)]!}{j![(m-j)!]^2}H_{2j}(y)=[H_m(2^{-1/2}y)]^2 ,$$

we finally obtain the well-known result[8,11,15]

$$W_m=\frac{2\sqrt{s}}{s+1}\left[\frac{s-1}{s+1}\right]^m(2^mm!)^{-1}\times\left[H_m\left[\frac{s}{(s^2-1)^{1/2}}\sqrt{2}\alpha\right]\right]^2\exp\left[-\frac{2s}{s+1}\alpha^2\right].$$

APPENDIX D: INTEGRATION OF WIGNER FUNCTION OVER A PATH IN PHASE SPACE

Any Wigner function $P^{(w)}_{|\psi\rangle}$ of a state $|\psi\rangle$ described by a wave function $\psi=\psi(x)$ has the remarkable property[6,7] to yield the probability distribution $|\psi(x)|^2$, when integrated over the dynamically conjugate variable p, that is,

$$\int_{-\infty}^{\infty}dp\,P^{(w)}_{|\psi\rangle}(x,p)=|\psi(x)|^2 . \tag{D1}$$

In this appendix we analyze the results of an integration over only part of p. Moreover, we focus on the Wigner function $P^{(w)}_m$ of (4.2) for the harmonic oscillator in the mth state and calculate the "diamond" integral

$$I_m^{\rm diam}(x)\equiv\int_{\bar{p}_m(x)}^{\infty}dp(-1)^me^{-(x^2+p^2)}L_m[2(x^2+p^2)] \tag{D2a}$$

and the "ditch" integral

$$I_m^{\rm ditch}(x)\equiv\int_{-\bar{p}_m(x)}^{\bar{p}_m(x)}dp(-1)^me^{-(x^2+p^2)}L_m[2(x^2+p^2)] \tag{D2b}$$

for $|x|<\sqrt{2(m+\frac{1}{2})}$ in the large m limit.

We start with $I_m^{\rm diam}$. When we introduce the new variable $\rho\equiv2(x^2+p^2)$, Eq. (D2a) reduces to

$$I_m^{\rm diam}(x)=\frac{1}{4}\int_{\rho_m}^{\infty}d\rho\frac{(-1)^m}{\left[\frac{\rho}{2}-x^2\right]^{1/2}}e^{-\rho/2}L_m(\rho) ,$$

where ρ_m denotes the largest zero of the mth Laguerre polynomial.[18] We evaluate the slowly varying square root $(\rho/2-x^2)^{1/2}$ at the turning point[19] $\rho_t\cong4(m+\frac{1}{2})$ of $\exp(-\rho/2)L_m(\rho)$, factor it out of the integral, and arrive at

$$I_m^{\rm diam}(x)\cong\frac{1}{4}\frac{1}{p_m(x)}\int_{\rho_m}^{\infty}d\rho(-1)^me^{-\rho/2}L_m(\rho) .$$

Here we have used Eq. (2.6).

The remaining integral has been calculated in Ref. 21 in the limit $m \rightarrow \infty$ and yields

$$\int_{\rho_m}^{\infty} d\rho (-1)^m e^{-\rho/2} L_m(\rho) \cong 2 ,$$

and thus

$$I_m^{\text{diam}}(x) \cong \frac{1}{2} \frac{1}{p_m(x)} . \tag{D3}$$

We now turn to I_m^{ditch}, Eq. (D2b), and make use of Eq. (D1),

$$\int_{-\infty}^{\infty} dp\, P_m^{(w)}(x,p) = \int_{-\infty}^{\infty} dp \frac{(-1)^m}{\pi} e^{-(x^2+p^2)} \times L_m[2(x^2+p^2)] = u_m^2(x) .$$

For $|x| < \sqrt{2(m+\frac{1}{2})}$ the wave function u_m of the mth eigenstate, Eq. (2.3), can be approximated by the WKB wave function,[3] Eq. (2.5), and thus

$$(1/\pi) \int_{-\infty}^{\infty} dp (-1)^m e^{-(x^2+p^2)} L_m[2(x^2+p^2)] \cong \frac{1}{\pi} \frac{1}{p_m(x)} \left\{ 1 + \cos \left[2S_m(x) - \frac{\pi}{2} \right] \right\} . \tag{D4}$$

When we decompose the preceding integral and use the definitions, Eq. (D2), we find

$$\int_{-\infty}^{\infty} dp (-1)^m e^{-(x^2+p^2)} L_m[2(x^2+p^2)] = 2 I_m^{\text{diam}}(x) + I_m^{\text{ditch}}(x) . \tag{D5}$$

With the help of Eq. (D3) we thus conclude from Eqs. (D4) and (D5)

$$I_m^{\text{ditch}}(x) \cong \frac{\cos \left[2S_m(x) - \frac{\pi}{2} \right]}{p_m(x)} . \tag{D6}$$

The inner wave troughs and crests of $P_m^{(w)}$ are therefore related to the oscillatory part of the wave function, $\cos(S_m - \pi/4)$, whereas the outermost crest can be associated with the classical probability[4,14]

$$P_m^{(\text{classical})} = \text{const}/p_m(x) .$$

---

[1]For the central role of the double-slit experiment in quantum mechanics, see, for example, R. P. Feynman, R. B. Leighton, and M. Sands, *The Feynman Lectures on Physics* (Addison-Wesley, Reading, MA, 1964), Vol. 3; or the famous Bohr-Einstein dialogue, reprinted and commented on in J. A. Wheeler and W. H. Zurek, *Quantum Theory and Measurement* (Princeton University Press, Princeton, 1983).

[2]The importance of probability amplitudes rather than probabilities is emphasized in the path-integral formulation of quantum mechanics. See, for example, R. P. Feynman and A. R. Hibbs, *Quantum Mechanics and Path Integrals* (McGraw-Hill, New York, 1965); L. S. Schulman, *Techniques and Applications of Path Integration* (Wiley, New York, 1981).

[3]P. Debye, Physik. Zeitschr. **28**, 170 (1927); W. Pauli, in *Die allgemeinen Prinzipien der Wellenmechanik,* Vol. 24 of *Handbuch der Physik,* edited by H. Geiger and K. Scheel (Springer, Berlin, 1933); H. A. Kramers, in *Quantentheorie des Elektrons und der Strahlung,* Vol. 2 of *Hand- und Jahrbuch der Chemischen Physik* (Eucken-Wolf, Leipzig, 1938).

[4]See, for example, M. Born, *Vorlesungen über Atommechanik,* in *Struktur der Materie in Einzeldarstellungen,* edited by M. Born and J. Franck (Springer, Berlin, 1925); R. L. Liboff, Phys. Today **37** (2), 50 (1984).

[5]The concept of interference in phase space is explained in J. A. Wheeler, Lett. Math. Phys. **10**, 201 (1985); W. Schleich and J. A. Wheeler (unpublished).

[6]For a review on Wigner distributions see, for example, M. Hillery, R. F. O'Connell, M. O. Scully, and E. P. Wigner, Phys. Rep. **106**, 121 (1984); V. I. Tatarskii, Usp. Fiz. Nauk. **139**, 587 (1983) [Sov. Phys.—Usp. **26**, 311 (1983)]; N. L. Balazs and B. K. Jennings, Phys. Rep. **104**, 347 (1984).

[7]The various distribution functions in phase space are reviewed by L. Cohen, in *Frontiers of Nonequilibrium Statistical Physics,* edited by G. Moore and M. O. Scully (Plenum, New York, 1986).

[8]For a review on squeezed states see, for example, D. F. Walls, Nature **306**, 141 (1983); **324**, 210 (1986); M. Nieto, in *Frontiers in Nonequilibrium Statistical Mechanics,* edited by G. Moore and M. O. Scully (Plenum, New York, 1986); see also the special issues on squeezed states in J. Opt. Soc. Am. B **4**, No. 10 (1987); J. Mod. Opt. **34**, No. 6 (1987).

[9]The notion of a nonclassical state and nonclassical distance is advocated, for example, by M. Hillery, Phys. Lett. A **111**, 409 (1985); Phys. Rev. A **31**, 338 (1985); **35**, 725 (1987).

[10]See, for example, W. H. Louisell, *Quantum Statistical Properties of Radiation* (Wiley, New York, 1973); or M. Sargent, M. O. Scully, and W. E. Lamb, Jr., *Laser Physics* (Addison-Wesley, Reading, MA, 1974).

[11]W. Schleich and J. A. Wheeler, Nature **326**, 574 (1987); W. Schleich and J. A. Wheeler, in *The Physics of Phase Space,* edited by Y. S. Kim and W. W. Zachary (Springer, New York, 1987); Ver. Dtsch. Phys. Ges. (VI) **22**, Q15.3 (1987); J. Opt. Soc. Am. B **4**, 1715 (1987); A. Vourdas and R. M. Weiner, Phys. Rev. A **36**, 5866 (1987).

[12]P. Drummond and D. F. Walls (unpublished).

[13]For a nice presentation of the Wigner function of the harmonic oscillator see, for example, J. R. Klauder, Bell Sys. Tech. J. **39**, 809 (1960).

[14]D. Bohm, *Quantum Theory* (Prentice-Hall, Englewood Cliffs, NJ, 1951).

[15]For the sake of simplicity we confine our discussion to minimum uncertainty squeezed states, such as that discussed in D. Stoler, Phys. Rev. D **1**, 3217 (1970); **4**, 1925 (1971); H. P. Yuen, Phys. Rev. A **13**, 2226 (1976).

[16]A. Sommerfeld, Sitzungsber. Münchner Akad. Wiss. 425 (1915); 459 (1915); Ann. Phys. (Leipzig) **51**, 1 (1916); M. Planck, Ann. Phys. (Leipzig) **50**, 385 (1916); P. Ehrenfest, *ibid.* **51**, 327 (1916).

[17]R. F. O'Connell and E. P. Wigner, Phys. Lett. **83A**, 145 (1981); R. F. O'Connell and A. K. Rajagopal, Phys. Rev. Lett.

48, 525 (1982); R. F. O'Connell and D. F. Walls, Nature **312**, 257 (1984); for an application of this relation to molecular collisions see H.-W. Lee and M. O. Scully, J. Chem. Phys. **73**, 2283 (1980).

[18]G. Szegö, *Orthogonal Polynomials* (American Mathematical Society, New York, 1939).

[19]F. Tricomi, *Vorlesungen über Orthogonalreihen* (Springer, Berlin, 1955).

[20]The semiclassical limit of the Wigner function has been considered in a multitude of publications; see, for example E. J. Heller, J. Chem. Phys. **67**, 3339 (1977); M. V. Berry, Philos. Trans. R. Soc. London **287**, 237 (1977); M. V. Berry and N. L. Balazs, J. Phys. A **12**, 625 (1979); H. J. Korsch, *ibid.* **12**, 811 (1979). It has been pointed out frequently that for most cases the Wigner function in the semiclassical limit can be expressed by an appropriately normalized δ function located at the Bohr-Sommerfeld phase-space trajectory, Eq. (3.1). For insight into when and why, see, especially, J. P. Dahl, in *Energy Storage and Redistribution in Molecules*, edited by J. Hinze (Plenum, New York, 1983); J. P. Dahl, in *Semiclassical Descriptions of Atomic and Nuclear Collisions*, edited by J. Bang and J. de Boer (Elsevier, Amsterdam, 1985).

[21]W. Schleich, H. Walther, and J. A. Wheeler (unpublished).

[22]I. S. Gradsteyn and I. M. Ryzhik, *Table of Integrals, Series and Products* (Academic, New York, 1965).

[23]W. Magnus, F. Oberhettinger, and R. P. Soni, *Formulas and Theorems for the Special Functions of Mathematical Physics* (Springer, New York, 1966).

[24]E. R. Hansen, *A Table of Series and Products* (Prentice-Hall, Englewood Cliffs, NJ, 1975).

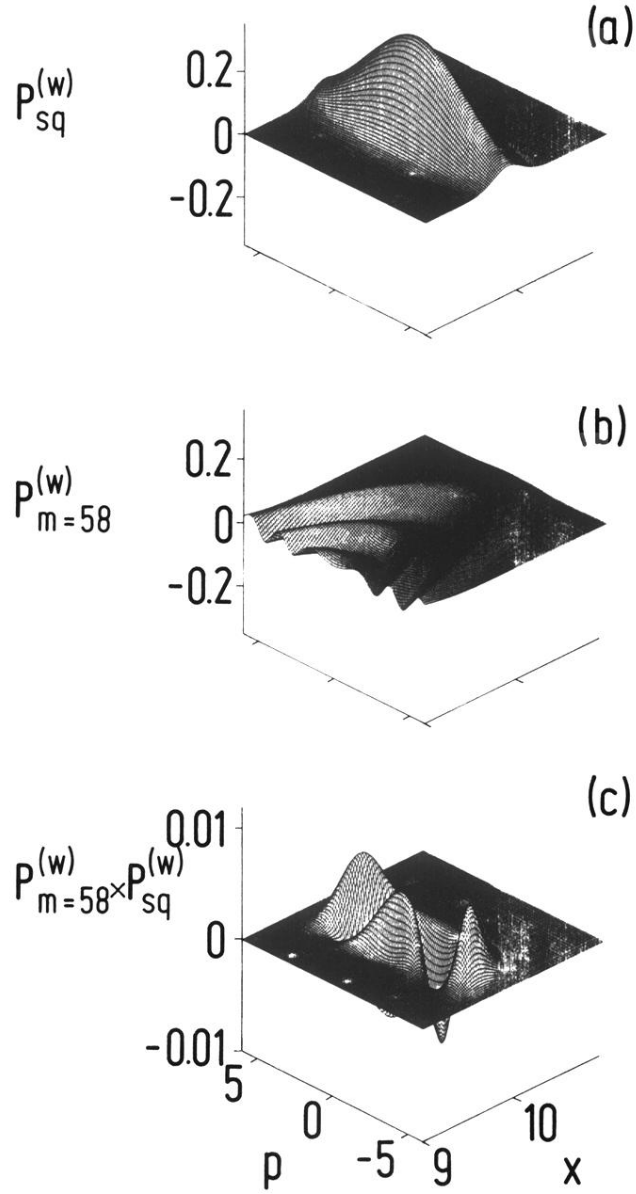

FIG. 3. In the framework of the Wigner function formalism the probability $W_{m=58}$ of finding $m=58$ photons in a highly squeezed state [Gaussian cigar of (a)] is obtained by integrating the product $P_{m=58}^{(w)}P_{\rm sq}^{(w)}$ of the corresponding Wigner functions (c) over phase space. In complete correspondence to the $m=58$th Bohr-Sommerfeld band of Fig. 2 the outermost wave front of the oscillator Wigner function $P_{m=58}^{(w)}$, (b), cuts out of the Gaussian cigar two symmetrically located peaks similar to the two diamond-shaped zones of Fig. 2. Moreover, the area $W_m^{\rm diam}$, underneath each of these peaks is equal to the area $A_m=\mathcal{A}_m$ of one of the weighted diamonds. The next inner wave front of $P_{m=58}^{(w)}$ exhibits negative values and creates a "ditch" in phase space and in the product $P_{m=58}^{(w)}P_{\rm sq}^{(w)}$. The following wave front with positive values gives rise to the "tongue," of (c). The weighted area of the "ditch" and the "tongue," $W_m^{\rm ditch}$, is given by Eq. (4.6′), $W_m^{\rm ditch} \cong 2\mathcal{A}_m\cos(2\phi_m)$, which results in the photon count probability $W_m = 2W_m^{\rm diam}+W_m^{\rm ditch} \cong 2\mathcal{A}_m+2\mathcal{A}_m\cos(2\phi_m)$. For $m=58$ we find roughly as many positively as negatively weighted areas and thus $W_{m=58}\cong 0$, in agreement with Fig. 1 (here we have chosen $\alpha^2=49$ and $\epsilon=0.1$).

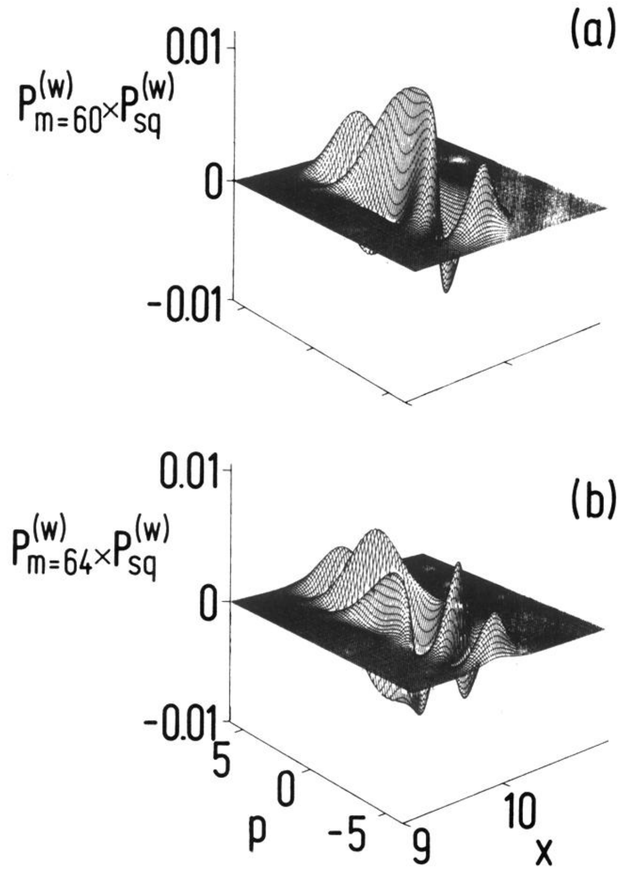

FIG. 4. When the field oscillator is in its $m=60$th state of excitation, the wave fronts have progressed further outwards compared to the $m=58$th state. Again the outermost band cuts out two symmetrically located peaks, each of weighted area $A_m = \mathcal{A}_m$. However, the following wave front with positive value now reaches deeper into the Gaussian cigar thus amplifying the "tongue" and reducing the depth of the "ditch," as shown in (a). Consequently, integration over phase space yields an unusually large value for $W_{m=60}$, in agreement with Fig. 1. This inner wave front has marched even further outwards for the $m=64$th state as to cut the Gaussian cigar twice. Only a small "tongue" survives from the next wave front with positive values. Therefore integration over phase space results in an almost vanishing probability $W_{m=64}$ as shown in Fig. 1. This clearly demonstrates that the oscillations in the photon distribution of a highly squeezed state result from the inner negative-valued wave fronts of the Wigner function for the oscillator. (Here, as in the other figures, we have chosen $\alpha^2=49$ and $\epsilon=0.1$.)